Rapamycin allosterically inhibits the proteasome

Pawel A. Osmulski and Maria Gaczynska

University of Texas Health Science Center at San Antonio, Department of Molecular

Medicine, Institute of Biotechnology, 15355 Lambda Drive, San Antonio, TX, 78245

Running title: **Rapamycin allosterically inhibits the proteasome**

Corresponding author: Maria Gaczynska

Address:

University of Texas Health Science Center at San Antonio, Department of

Molecular Medicine, Institute of Biotechnology, 15355 Lambda Drive, San

Antonio, TX, 78245

Tel.   (210) 567-7262

Fax: (210) 567-7269

E-mail: Gaczynska@uthscsa.edu

Number of text pages:

Number of tables: 1

Number of figures: 6

Number of references: 35

Number of words in *Abstract*:   211

Number of words in *Introduction*:   758 (without citations)

Number of words in *Discussion*:   1468

Nonstandard abbreviations: 5AHQ, 5-amino-8-hydroxyquinoline; AMC, 7-amino-4-methylcoumarin; Boc, butoxycarbonyl; Cbz, carbobenzoxy; ChT-L, chymotrypsin-like or post hydrophobic residues activity; CP, core particle; FKBP12, FK-binding protein 12; Hb, hydrophobic amino acid residue; MCA, 7-amido-4-methylcoumarin; mTOR, mammalian target of rapamycin; PA, proteasome activator; PGPH, post-glutamyl peptide hydrolyzing or post acidic residues activity; REG, regulator; RP, regulatory particle; Rpt, regulatory particle ATPases; S, Svedberg sedimentation units; Suc, succinyl; T-L, trypsin-like or post basic residues activity.

Abstract

Rapamycin is a canonical allosteric inhibitor of the mTOR kinase with immunosuppressive and pro-apoptotic activities. We found that *in vitro* rapamycin also regulates the proteasome, an essential intracellular protease of the ubiquitin-proteasome pathway. Rapamycin inhibits proteinase and selected peptidase activities of the catalytic core proteasome at low micromolar concentrations. Moreover, the drug interferes with binding of the 19S cap essential for processing of polyubiquitinylated substrates, and the PA200 activator to the 20S catalytic core proteasome. These protein complexes are known to bind to specific grooves on the α face region of the 20S core. A treatment with rapamycin affects conformational dynamics of the proteasomal gate, a centrally positioned within the α face and allosterically regulated element responsible for the intake of substrates. Interestingly, we showed that rapamycin shares all the proteasome targeting properties not only with other two-domain, closed-ring analogs (rapalogs), but also with its single domain mimics, and with *seco*-rapamycin. The latter is the first *in vivo* open-ring metabolite of rapamycin that does not affect mTOR. We hypothesize that the rapamycin and related compounds bind to the α face and allosterically impact the proteasome function. The implications of our finding for mechanism of *in vivo* actions of rapamycin and for design of novel allosteric drugs targeting the proteasome are discussed.

Introduction

The phenomenon of allostery, broadly defined as coupling of conformational changes between distant sites, is one of fundamental regulatory mechanisms of enzymatic catalysis (Goodey and Benkovic, 2008). Therefore, it comes to no surprise that allosteric ligands are rapidly gaining recognition as attractive drug candidates. In fact, allosteric inhibitors exhibit many benefits over the commonly utilized competitive inhibitors. They provide a much broader range of mechanisms to interfere with catalysis, are more specific and less likely to induce drug resistance. Still, the structural and functional complexity of many enzymes poses a special challenge in finding or designing allosteric regulators. One of such enzymes is the proteasome, the essential protease of the ubiquitin proteasome pathway, which plays critical regulatory and housekeeping functions in every eukaryotic cell (Ciechanover, 2012). Inhibition of proteasome leads to apoptosis, a feature already applied for cancer treatment (Adams, 2004). Several competitive proteasome inhibitors are used in humans, including two FDA-approved drugs: bortezomib/Velcade® and carfilzomib/ Kyprolis[TM] (Dick and Fleming, 2010). Apart from cancer, the proteasome is considered as a target for anti-inflammatory drugs (Tan et al., 2006).

The proteasome is a multifunctional and modular protease (Groll et al., 1997; Unno et al., 2002). Three pairs of its active sites are concealed inside the tube-shaped catalytic core (core particle; CP, 20S; Fig. 1A). The sites exhibit chymotrypsin-like (ChT-L), trypsin-like (T-L) and post-acidic (PGPH; post-glutamyl peptide hydrolyzing) specificities cleaving polypeptides after hydrophobic, basic and acidic amino acid residues, respectively. The activity of the CP is controlled by attachment of additional

protein modules to the external surface on both sides of the 20S. The surface (α face) harbors the gate guarding access to the catalytic chamber and accepts 19S regulatory particle (RP), 11S (PA28/REG; proteasome activator/regulator) or PA200 activators (Fig. 1B-D). A complex of the core with one or two (26S proteasome) 19S "caps" recognizes and processes substrates tagged for degradation by polyubiquitinylation (Da Fonseca et al., 2012; Huber and Groll, 2012; Lander et al., 2012; Lasker et al., 2012). Proteins decorated with polyubiquitin comprise the majority of proteasomal substrates *in vivo*. The regulatory modules anchor in grooves between α subunits (Fig. 1A), with the module-specific effects and mechanisms of binding allosterically affecting catalytic activity of the proteasome. Their attachment is accompanied by opening of the gate and by shifts in peptidase specificities (Bajorek et al., 2003; Rechsteiner and Hill, 2005). However, gate opening is mediated not only by signals from the grooves on the α face, but also by signals from the catalytic chamber (Osmulski et al., 2009; Rabl et al., 2008; Whitby et al., 2000). Besides gate regulation, the allosteric path between active sites and the α face is utilized for modulation of stability of the 26S assembly (Kleijnen et al., 2007).

Contrary to competitive inhibitors, the small-molecule allosteric ligands of the proteasome are much less explored. There is an example of an allosteric inhibitor, 5-amino-8-hydroxyquinoline (5AHQ) binding inside the antechamber (Li et al., 2010). On the other hand, Pro and Arg rich (PR) peptides bind to the α face, likely on its outer edge, destabilize the gate and the RP-CP interactions, and affect peptidase activities *in vitro* (Gaczynska et al., 2003). *In vivo*, PR peptides inhibit degradation of selected

substrates and display anti-inflammatory and pro-angiogenic properties (Gao et al., 2000; Li et al., 2000).

The phenomenon of regulation of the core properties by attachment of dedicated proteins to specific allosteric sites inspired us to search for small molecule allosteric ligands affecting protein-protein interactions. A straightforward case of such interference is provided by short peptide sequences derived from C-termini of the modules, blocking the grooves and mimicking some allosteric effects of their parent proteins (Jankowska et al., 2010). The anchor peptide fragments of selected Rpt (regulatory particle ATPases) subunits of the 19S, and of PA200 activator, are equipped with the Hb-Y-X motif (hydrophobic amino acid-Tyr-any amino acid) (Ortega et al., 2005; Rabl et al., 2008). We hypothesized that a canonical hydrophobic allosteric ligand such as rapamycin may interfere with the docking of protein modules to the α face and may provide alternative to the short peptides.

Indeed, rapamycin (sirolimus) is one of the oldest examples of a successful allosteric drug. This natural macrocyclin binds the FKBP12 (FK-binding protein 12) with its FKBP binding domain, induces dimerization of FKBP12 and mTOR (mammalian target of rapamycin) and inhibits the latter with its effector domain binding to the allosteric side adjacent to the kinase domain (Fig. 2) (Banaszynski et al., 2005; Liang et al., 1999). The mTOR kinase regulates translation, autophagy, response to hypoxia, and glucose metabolism (Dowling et al., 2009). Rapamycin is an immunosuppressive drug used to prevent transplant rejection. High doses of the drug are pro-apoptotic and close synthetic analogs of rapamycin (rapalogs) are used as anti-cancer agents (Dowling et al., 2009). In addition, animal studies revealed surprisingly strong anti-aging

effects of a prolonged treatment with low doses of rapamycin (Harrison et al., 2009).

Here we report a discovery that rapamycin, rapalogs and a rapamycin metabolite are allosteric regulators of the core proteasome. They interfere with substrate gating and with interactions between the 20S core and 19S components. The discovery opens opportunity to design a new class of allosteric proteasome inhibitors targeting allosteric sites on the α face and possessing potential anticancer properties.

Materials and Methods

Proteasome activity measurements

Human purified proteasome complexes were purchased from Enzo LifeSciences (20S and 26S) or Boston Biochemicals (19S complex). BODIPY-casein (Invitrogen/Molecular Probes) was used as a model protein substrate, with increasing fluorescence of BODIPY labeled peptide products of degradation monitored for up to 8 hours at 37°C. The peptidase activity of the enzyme was measured as arbitrary intensity units of the released fluorescent group 7-amino-4-methylcoumarin (AMC) from peptide substrates, as described. The common substrates specific for the three kinds of active sites: succinyl-LeuLeuValTyr-7-amido-4-methylcoumarin (Suc-LLVY-MCA; for the ChT-L activity; Bachem), butoxycarbonyl-LeuArgArg-MCA (BocLRR-MCA; for T-L; Bachem) and carbobenzoxy-LeuLeuGlu-MCA (CbzLLE-MCA; for PGPH; Enzo Life Sciences International, Inc.) were used at 100 μM final concentrations, unless stated otherwise (Gaczynska and Osmulski, 2005). Proteasome substrates, rapamycin, its derivatives, and competing peptides were stocked in DMSO and diluted 100-fold in the reaction mixtures. The Rpt5 and PA200 C-terminal peptides were synthesized in the Departmental Peptide Synthesis Core using the standard SPPS chemistry. To activate the latent 20S proteasome, 0.005% (final concentration) of sodium dodecyl sulfate (SDS) was used. The reactions were carried out in 96 well plates, with 2.3 nM proteasome and other components as indicated dissolved in 50 mM Tris-HCl buffer (pH 8.0) and incubated at 37°C for up to 1 hour. To study reconstruction of the 26S proteasome with 20S and 19S complexes, the reaction buffer was supplemented with 2

mM ATP, 1 mM MgCl$_2$ and 1mM DTT. The fluorescence of released AMC was monitored every 2 minutes with a Fluoroskan Ascent plate reader. Reaction rates were calculated from smoothed linear segment of kinetic curves using OriginPro 8.6 (OriginLabs, Northampton, MA). For the determination of an inhibition type, at least six distinct substrate concentrations and two inhibitor concentrations were used. The kinetic parameters of inhibition were analyzed in terms of the Michaelis-Menten formalism using the enzyme kinetic module of SigmaPlot v.12 (Systat Software, Inc, San Jose, CA) to perform the respective calculations.

Atomic force microscopy imaging

AFM imaging of the 20S proteasomes was performed in tapping (oscillating) mode in liquid, as previously described (Gaczynska and Osmulski, 2011; Osmulski et al., 2009). In short, 3 μL of proteasome preparations diluted to nanomolar concentration were deposited on a freshly cleaved muscovite mica surface. After 2 min incubation allowing electrostatic attachment of the protein particles to mica the droplet was overlaid with 30 microL of 50 mM Tris-HCl buffer (pH 7.0) and mounted in the wet chamber of a MultiMode NanoScope IIIa (Bruker Corp.). Oxide-sharpened silicon nitride tips on cantilevers with a nominal spring constant 0.32 N/m (Bruker Corp.) were used to image 1 μm^2 fields in the height mode, with a scan rate of 3.05 Hz. The excitation frequency was manually tuned to 9-10 kHz, with a drive voltage of 200-500 mV and a relatively high set point (1.6 V to 1.9 V) to assure tapping with low, non-destructive force. Trace and retrace images were collected with resolution of 512 x 512 pixels, which resulted in a digital (apparent) resolution of 2 nm in x and y directions. As we established

previously, such resolution was sufficient to detect distinct conformations of the α face, covered by six scan lines. Multiple fields were scanned for each sample to collect images of hundreds of particles. Selected fields were repeatedly scanned to monitor changes in topography of the same particles for prolonged time. Inhibitors and the SucLLVY-MCA substrate were diluted in 10 μL of the imaging buffer and directly injected into the chamber. Raw images are presented, with a standard plain-fit and flattening (NanoScope software v.5.12) used as the only processing tools. For display purposes the brightness and contrast of the images was adjusted with the Nanoscope software or with Adobe Photoshop (Adobe Systems Inc.), and outlier scan lines were occasionally manually removed (Nanoscope software). Top view ("standing", rounded) proteasomes were distinguished from the minor population of side-view ("lying", rectangular) particles as described, by comparison of their length – to width ratios (Osmulski et al., 2009). The dimensions of particles were approximated and a shape of the α face in top-view proteasomes was judged with the help of a section tool in the Nanoscope v.5.12 or SPIP v.6.02 software (Image Metrology).

Results

Rapamycin noncompetitively inhibits proteolytic activity of the 20S proteasome.

The core proteasome (CP) particle is capable of cleaving short peptides and poorly structured proteins, for example certain transcription factors with intrinsically disordered domains, or proteins partially unfolded by stressors. The free CPs are believed to exist

in a cell where they are involved in ubiquitin-independent degradation of selected disordered or damaged substrates (Liu et al., 2003; Pickering et al., 2010). *In vitro*, the poorly folded protein such as casein can be used as a model substrate for the 20S proteasome. We tested the influence of rapamycin on degradation of fluorescently labeled casein by the latent proteasome. An addition of 2 μM or 5 μM rapamycin slowed down the release of fluorescent products 2 to 3 – fold (Fig. 3). Moreover, for the drug-treated proteasomes the release of new products almost ceased after 1 hour of incubation, whereas for the control enzyme accumulation of products continued for at least 8 hours. Since degradation of protein engages all active sites of the proteasome, to gain insight into the effects of rapamycin on the performance of individual active sites we tested degradation of site-specific short peptide substrates. Rapamycin inhibited post-hydrophobic and post-acidic peptidase activities of the purified latent human proteasome in sub-micromolar to low micromolar concentrations, with IC_{50} (concentration of an inhibitor inducing a 50% decrease of the maximal enzyme reaction rate) of 1.9 μM and 0.4 μM, respectively (Table 1). Titration curves of ChT-L peptidase inhibition obtained for housekeeping and immunoproteasome were undistinguishable (not shown); consequently we used the housekeeping 20S in all subsequent experiments. Consistent with previously reported data (Meyer et al., 1997), the detergent-activated CP was refractory to rapamycin up to concentration of about 5 μM, with only a weak inhibition of post-hydrophobic cleavages noted at higher drug concentrations. The interactions between 20S and rapamycin were fully reversible. Incubation of CP with 2 μM rapamycin lowered the ChT-L peptidase activity to 51%±2%. After a 10-fold dilution, the ChT-L peptidase was 100%±12% active, as compared with

11

the control treated with DMSO. The inhibition effect was reversible in the case of the PGPH peptidase as well. Namely, incubation of CP with 0.5 μM rapamycin lowered the PGPH peptidase activity to 49%±6% and the activity rebound to 91%±6% (means±SD; n=3) of the control after a 10-fold dilution of the reaction mixture.

Analysis of peptide degradation in the presence of rapamycin indicated a mixed type of inhibition mechanism for the ChT-L peptidase (Fig. 4A). On the other hand, the pure noncompetitive inhibition was found for the PGPH peptidase (Fig. 4B). Similarly to certain other small noncompetitive ligands of the proteasome, the actions of rapamycin were not restricted to inhibition of the peptidases (Jankowska et al., 2010). The T-L peptidase was moderately activated by rapamycin. The activation of post-basic cleavages was of nonessential type, with nearly two-fold increase in activity and with the K_d in the range of 0.1 μM (Fig. 4C, Table 1).

Rapamycin derivatives and a rapamycin metabolite affect the activities of 20S proteasome

As a next step in our analysis we tested effect of rapamycin-derived small ligands known as mTOR inhibitors. Modifications of rapamycin introduced on carbon-40 (temsirolimus, everolimus, and ridaforolimus), which is not directly involved in interactions with mTOR or FKBP12 (Fig. 2A), did not abolish the inhibition of the proteasome. The IC_{50} values for rapalogs were not much different from the IC_{50} values recorded for rapamycin. They tend to be slightly higher than for rapamycin in the case of the ChT-L peptidase, and very similar in the case of PGPH peptidase (Table 1). It is worth to mention that temsirolimus (Torisel) and everolimus (Afinitor) are in clinical trials

as anti-cancer drugs (Vignot, 2005). The rapalogs modified at the C-40 position retain the binding and effector domains that are two pharmacophores characteristic for rapamycin (Fig. 2A). In contrast, single domain rapamycin mimics such as pimecrolimus and FK-506 preserve only the FKBP binding domain (Fig. 2B). Nevertheless, both the compounds inhibited the two peptidase activities of the proteasome, albeit less efficiently than rapamycin or rapalogs (Fig. 4D, Table 1). The inhibition of post-acidic cleavages was the least affected by the lack of effector domain, with the IC_{50} increasing by only 40% in the case of pimecrolimus as compared with rapamycin (Table 1). At low concentrations of the drugs, up to about 1 µM, the two-domain (rapamycin) and single domain (FK-506) derivatives inhibited the ChT-L activity to similar extent (Fig. 4D). However, treatment with 10 µM rapamycin lowered the activity to 30% or less, whereas effects of 10 µM FK-506 and pimecrolimus remained at the 50%-60% level. On the other hand, the PGPH activity was routinely lowered to 10% -15% by all the drugs at 10 µM concentration (Fig. 4E).

The two single-domain mimics activated the T-L peptidase even stronger than rapamycin. However, they reached the maximal effects at relatively high concentrations (Fig. 4F, Table 1).

In addition to two-domain analogs and single-domain mimics, we tested *seco*-rapamycin, the open-ring first product of rapamycin metabolism in humans (Fig. 2C). *Seco*-rapamycin was reported not to affect the mTOR function (Cai et al., 2007). Surprisingly, the metabolite did affect the proteasome activities at the low micromolar concentrations, with the PGPH and T-L peptidases affected the most. The efficiency of inhibition or activation by *seco*-rapamycin was lower than by rapamycin, but still only 5

13

µM of the former was sufficient to induce nearly a 50% inhibition of the post-acidic cleavages or almost a 2-fold activation of post-basic (T-L) cleavages (Fig. 4F, Table 1). In contrast, all three proteasome peptidase activities were refractory to the treatment with up to 10 µM of PI-103 or NVP-BEZ235, the mTOR kinase inhibitors blocking its ATP-binding pocket that are structurally distinct from rapamycin (Fig. 2D, Table 1, legend).

Comparison of the IC_{50} values revealed interesting trends in the inhibition potency among the rapamycin-related compounds. The post-hydrophobic (ChT-L) cleavages were much better inhibited by the two-domain compounds than by the single-domain and linear derivatives (Fig. 4D, Table 1). When it came to post-acidic (PGPH) cleavages, both the two-domain and single-domain drugs were comparably good inhibitors, leaving the linear metabolite as a sole example of a weak inhibitor (Fig. 4E, Table 1). On the other hand, the significantly better maximal activation of the post-basic (T-L) cleavages was induced by the single-domain compounds. Surprisingly, the maximal T-L activation effect was observed at much lower concentrations of the two-domain drugs (Fig. 4F, Table 1). Summarizing, all the tested rapamycin-related compounds exerted diverse effects on the peptidase activities of human catalytic core proteasome. However, the efficiency of inhibition or activation was clearly related to the structural constrains of the rapamycin derivatives.

Rapamycin and its derivatives affect conformation of the proteasome α face.

The noncompetitive nature of inhibition by rapamycin prompted us to search for the compound induced structural changes in the core proteasome. For this purpose we used the noninvasive tapping mode atomic force microscopy (AFM) in liquid, the imaging technique suitable for analysis of surface topography of macromolecules in their native state with a nanometer-scale practical resolution. We established before that AFM imaging is an indispensable tool for studying structural dynamics of the 20S α face (Gaczynska and Osmulski, 2011; Gaczynska et al., 2003; Osmulski et al., 2009). Namely, we demonstrated that the gate of the latent, free core proteasome exists in a state of conformational equilibrium between the prevailing closed-gate state and the less populous open-gate state (Osmulski and Gaczynska, 2002). We assume that the open-gate conformation enables substrates to enter the central channel and to reach the catalytic chamber, and thus the AFM-detected sporadic gate opening accounts for the detectable catalytic activity of the latent 20S proteasome. We acquired and analyzed images of hundreds of single native, fully active 20S molecules. The majority of particles were in top-view ("standing") position conveniently allowing for imaging of their α faces. A closer analysis of the zoomed-in images of control human 20S proteasomes revealed the presence of two clearly distinguishable conformations: one with a smooth, cone-shaped α face, and another with a crater-shaped dip in the middle of α face, where the gate to the proteasome catalytic chamber is located. Following our previous extensive studies, we refer to the two forms as "closed-gate" and "open-gate" proteasomes, respectively (Osmulski et al., 2009). As described before, we used the shape of sections carried out in four directions through the top portion of the surface

15

topography of the α ring to distinguish between the two forms. In short, a particle was classified as closed if all four sections were cone-shaped. In contrast, the particle was classified as open if all sections presented a dip surrounded by a rim (Fig. 5A) (Gaczynska and Osmulski, 2011; Osmulski et al., 2009). The same particles imaged in consecutive scans were able to assume either closed or open conformations, however the cone-shaped particles were always more abundant than crater-shaped, and accounted for about three-quarters of the imaged molecules (Fig. 5B, C). Addition of rapamycin to the imaged particles remarkably changed the partition of forms. In the presence of rapamycin at concentrations as low as 0.2 μM, the closed forms accounted for 61% of proteasomes, a statistically significant (p<0.001) difference with the 75% closed CP registered for control proteasomes (Fig. 5D). The abundance of closed molecules decreased with increasing concentration of rapamycin reaching 40% at 10 μM of the drug, and was paralleled by decreasing activities of the ChT-L peptidase (Fig. 5D). The rapamycin-treated particles retained their ability to switch between forms, similarly to the control particles treated with DMSO (Fig. 5C). The derivatives of rapamycin followed the parent drug in the ability to change the conformational equilibrium. The exposure to 10 μM concentration of any of the three compounds: the linear metabolite (*seco*-rapamycin), the one-domain mimic (pimecrolimus) or the two-domain rapamycin resulted in a very similar ultimate partition of conformers reaching about 60% open and 40% closed proteasomes (Fig. 5E). The conformational shift from the 1 : 3 ratio in control to the 3 : 2 partition of open to closed particles, albeit highly significant, was still less pronounced than a shift to the 3 : 1 partition we observed before for eukaryotic proteasomes engaged in catalytic action under the steady state

conditions (Osmulski et al., 2009). Therefore, we tested if the presence of rapamycin would affect the catalysis-related changes in the partition of conformers. We added a model substrate for the post-hydrophobic peptidase to the 20S proteasomes already pretreated with rapamycin or its derivatives. Remarkably, the partition of conformers did not change significantly, in a sharp contrast with control proteasomes, which conformed to the expected 3 : 1 (open : closed) partition under the same conditions (Fig. 5E). We also checked a response of CP topography to a treatment with PI-103, which as a non-allosteric mTOR kinase inhibitor does not significantly affect the proteasome activities *in vitro.* Proteasomes treated with PI-103 were undistinguishable from the DMSO-treated control, and followed the response of control particles to the treatment with the substrate (Fig. 5E, caption and Table 1, legend).

All the compounds at 10 μM concentration induced almost the identical ultimate partition of the CP conformers what would suggest that CP achieved the maximum of structural response to the presence of the ligands detectable with AFM. In contrast, at this concentration each of the compounds also produced maximal but clearly a distinct level of peptidase inhibition (Fig. 5F).

Rapamycin and related compounds interfere with activation of the 20S core by 19S but not 11S regulators.

As demonstrated above, rapamycin interfered with dynamics of the proteasome gate located on the α face. This result inspired us to test if the drug would affect interactions of the 20S core with the 19S regulatory particle, which binds to the α face. *De novo* assembly of 19S from subunits is a complex process assisted by chaperones. *In vitro*,

and likely also in cells, the 26S can also be reconstructed from 20S and the already-assembled 19S particle in the presence of ATP (Smith et al., 2005). Enhancement of the peptidase activities of the core proteasome is an established test for efficiency of the *in vitro* reconstruction. Addition of RP to CP at the 1:1 molar ratio resulted in a two-fold increase of the ChT-L activity. In contrast, a pretreatment of 20S with 5 μM rapamycin before adding ATP and 19S totally abrogated the activation, leaving the proteasome almost 40% inhibited instead (Fig. 6). The activities of already assembled 26S proteasome were not significantly affected by rapamycin (see below) and related compounds (compounds listed in Table 1; data not shown) at up to 10 μM concentrations. For example, the relative ChT-L activity of the 26S treated with 1, 2, 5 or 10 μM rapamycin was 103%±14%, 103%±6%, 105%±9%, 111%±4%, respectively (mean±SD, n= 3 or 4). In a representative experiment the relative ChT-L activity of the 26S treated with 10 μM of rapamycin derivatives was 107% (temsirolimus), 101% (everolimus), 104% (ridaforolimus), 108% (FK-506), 94% (pimecrolimus), and 96% (seco-rapamycin) in comparison with the activity of the solvent only (DMSO) treated 26S proteasome (100%). The specific activity of the 26S preparation used in the experiments was 0.74±0.09 nanomol of AMC/mg per sec (n=5), and was about 4-fold higher than the specific activity of the 20S (Fig. 6, legend).

Interestingly, the interference of rapamycin with the peptidase activation was not restricted to the interactions of CP with the entire 19S particle. It is established that the activation of CP by RP can be reproduced by C-terminal peptides derived from the selected ATPase subunits of the 19S. It has been determined previously that a 10 residue long peptide derived from the C-terminal segment of Rpt5 (tRpt5; Fig. 2D)

exhibits the strongest activating effect. We decided to test the influence of rapamycin on the activation imposed by tRpt5. Addition of 10 μM tRpt5 resulted in a more than 2-fold increase in the core proteasome activity. However, when the CP was pretreated with 5 μM rapamycin before addition of the 10 μM tRpt5, the activation was totally abolished, and the CP was mildly inhibited instead (Fig. 6). The tRpt5 was not the sole core-activating peptide derived from protein ligands attaching to the α face. The 10-residue C-terminal fragment of the activator protein PA200 (tPA200; Fig 2B) shares with tRpt5 the capability to activate CP. Again rapamycin was abolishing the activation by the 10μM tPA200 peptide. Addition of 10μM rapamycin left the proteasome 50% inhibited instead of 2-fold activated (Fig. 6). The above trends were observed for the single-domain rapamycin mimic (FK-506) and the open metabolite (*seco*-rapamycin) as well. Their effects were the most pronounced in the presence of the tPA200: an addition of the 10 μM derivatives caused about 40% inhibition of the proteasome regardless the presence or absence of the 10 μM tPA200. FK-506 and *seco*-rapamycin interfered with activation of the core by the tRpt5 peptide, albeit not as efficiently as rapamycin. Upon treatment with either derivative (10 μM), the activation by the peptide (10 μM) was still well detectable, however it was about 30% lower than without the inhibitors. To the contrary, no detectable effects on activation of 20S with 19S were observed upon treatment with 5 μM PI-103.

Not all α face ligands were sensitive to the presence of rapamycin. An incubation of the CP with the heterohexameric PA29αβ/REGαβ (11S) at the 1:1 molar ratio increased the ChT-L peptidase activity 8-fold. The activation level remained unaffected upon an addition of 5 μM rapamycin before fortifying CP with the 11S complex (Fig. 6).

Summarizing, rapamycin and its derivatives influenced functional effects of selected ligands of the α face, including the most physiologically relevant 19S regulatory particle.

Discussion

Here we report that rapamycin, a canonical inhibitor of the mTOR kinase, affects *in vitro* performance of the 20S proteasome, the major intracellular protease in human cells. Rapamycin compromises degradation of the model protein, attenuates two out of three major peptidase activities, and interferes with interactions of the 20S with its physiological regulators.

Rapamycin and all the related compounds, regardless of their macrocyclic structure productively interact with the proteasome. It was rather surprising that the effector domain of rapamycin, missing in the single-domain derivatives is only a beneficial but not essential factor for proteasome targeting. Even more remarkable, the presence of the closed macrocyclic structure, essential for targeting the mTOR pathway, is dispensable in the case of proteasome targeting. Nevertheless, the macrocycle likely enforces the conformation supporting the most productive interactions with CP. Since effects of each rapamycin-related compound on the individual activities are qualitatively similar, it is plausible that all of them utilize the same binding sites. Taken together, the data demonstrate the possibility to design rapamycin-inspired compounds targeting the proteasome without directly influencing the mTOR pathway, a case represented here by *seco*-rapamycin.

Our data strongly support the hypothesis that a significant part of the observed functional effects of the rapamycin related compounds on proteasome are allostery driven. The diversity of effects exerted on the peptidase activities: pure noncompetitive inhibition, mixed type inhibition or moderate activation, provides the first culprit. We noted similarly diverse effects before with allosteric ligands of the 20S core: PR peptides and peptide fragments of proteins binding to the proteasome (Gaczynska et al., 2003; Jankowska et al., 2010). The AFM detected rapamycin induced changes in dynamics of the gate offer an additional line of evidence for the allosteric nature of rapamycin actions. We already used AFM imaging of the proteasome α face to identify gate movements allosterically driven by structural changes in the active centers or to detect conformational destabilization of the α face induced by PR peptides (Gaczynska et al., 2003; Osmulski et al., 2009).

Analysis of AFM images revealed that a treatment with rapamycin induces in a dose-dependent manner a shift of the conformational equilibrium toward moderately elevated incidence of the open-gate state. The frequency of the open gate CP is significantly higher than in the latent proteasome but substantially lower than in the proteasome engaged in catalytic action. Importantly, the abundance of the open conformers in the rapamycin treated proteasomes is refractory to an addition of the excess of a peptide substrate. The lower abundance of the open conformers likely compromises substrate gating and prevents the CP from reaching its full catalytic potency. Rapamycin and its allies thus emerge as unique regulators affecting conformational dynamics of the target enzyme.

However, it seems that the perturbations of substrate gating amount for just a part of the inhibitory effects of the agents. Interestingly, the same partition of proteasome conformers induced by the high dose of distinct rapamycin derivatives result in very distinct levels of peptidase inhibition that clustered according to the number of the domains and preservation of the macrocycle. Moreover, the "maximal inhibitory effects" were in perfect agreement with the drugs' IC_{50} values. Overall, the two canonical pharmacophore domains are required to reach the strong inhibition of the ChT-L peptidase. On the other hand, the presence of only FKBP binding domain is sufficient for the effective inhibition of the PGPH peptidase. We hypothesize that interactions of the proteasome with all the tested rapamycin-related compounds induce the maximal conformational shift resulting in the compromised gating of substrates. These effects manifest in the weak-to-moderate inhibition of ChT-L and PGPH activities by *seco*-rapamycin. However, the FKBP binding domain in pimecrolimus and rapamycin enables interaction with a putative allosteric site responsible for strong inhibition of the PGPH activity. The effector domain as a second pharmacophore present in rapamycin might be engaged in additional interactions leading to a stronger attenuation of the ChT-L peptidase. Thus, the inhibition exerted by pimecrolimus and rapamycin would be a cumulative effect of the gate opening and inhibition via additional allosteric routes. The hypothesis would accommodate well the differences in inhibition type of the ChT-L and PGPH peptidases. The pure noncompetitive inhibition of post-acidic cleavages may stem from interactions of two pharmacophores with the 20S proteasome: the putative pharmacophore present in all the studied rapamycin derivatives regardless of cyclization, and the FKBP binding domain of the cyclic compounds. The mixed-type

inhibition of post-hydrophobic cleavages would then require yet additional pharmacophore, the effector domain, perhaps responsible for the competitive-like component in the inhibition mechanism. Without additional structural studies it is impossible to decide if the compounds bind to one or more sites, and if binding to a single site affects one or more allosteric routes. Nevertheless, the data point at the importance of protein dynamics in biological catalysis, an emerging concept of great implications for the rational drug design and for protein engineering.

Identification of binding sites of rapamycin and its derivatives with the proteasome core demands extensive structural studies. However, we found that rapamycin and related compounds abrogate activation of the core by protein and peptide ligands known to anchor in the grooves on the α face. Therefore, we may speculate that rapamycin directly competes with canonical ligands for the same binding grooves, which are already allosterically connected to the gate and, putatively, to the catalytic chamber. These links can be utilized by rapamycin. Indeed, the molecular modeling data fully support effective docking of rapamycin to at least selected grooves (Boehner, Gaczynska, Osmulski, unpublished observations). Rapamycin binding apart from the grooves or even apart from α face still cannot be excluded; however it would entail the presence of new potential binding sites and yet-unknown allosteric connections.

Interestingly, rapamycin does not interfere with activation of the core by the 11S particle, thus limiting the effective competition to ligands utilizing the Hb-Y-X motif for binding. The proteasome activator/regulator PA28/REG anchors in the grooves with C-termini devoid of Hb-Y-X, however the interactions are stabilized by activation loops

(Whitby et al., 2000). We may envision that the 11S heptamer efficiently blocks access to all grooves on the occupied α face, unlike the peptide ligands or, possibly, the wobbling – prone 19S cap. The results, however, suggest a more complex effect than a simple outcompeting the rapamycin by 11S activator. Even when 11S was added to the 20S in a 1:1 molar ratio, not sufficient to saturate the CP, the peptidase activity was not affected by rapamycin. This result can be explained by the following non-excluding phenomena. First, binding the 11S may allosterically lower the affinity of the core to rapamycin, or may abrogate the inhibitory effects of rapamycin already bound to the core. Second, adding rapamycin may result in a partition of 20S, 20S-11S and 11S-20S-11S complexes, which is very distinct from that established in the absence of the drug. The shifts in partition resulting in specific alterations in activity may effectively obscure the inhibition by rapamycin. The experiments determining potential rapamycin-induced changes of 20S affinity to the protein regulators are under way.

The presented data demonstrate that rapamycin, its derivatives, and its metabolite are unexpected inhibitors of the CP. They likely utilize a novel molecular mechanism of action involving allosteric interactions. *In vitro*, they interfere with gating of substrates and with binding of the physiologically critical 19S assembly. There are two important questions concerning practical implications of the finding. First, does the effect have any significance *in vivo*, in humans or animals treated with rapamycin or rapalogs? Second, can the unique mechanism of action be of pharmacological use? The *in vitro* affinity of rapamycin and rapalogs to mTOR is much higher than to the proteasome, with IC_{50} difference in a range of at least two orders of magnitude. We could expect that *in vivo* consequences of mTOR inhibition will be evident with much

lower dose of the drug than any direct effects on the proteasome. However, our observation that *seco*-rapamycin exerts significant effects on the proteasome *in vitro* while not affecting mTOR *in vivo* opens a venue for design of compounds inspired by the structure of rapamycin and seco-rapamycin but specifically targeting the proteasome with the new allosteric mechanism. We may speculate that such compounds will have distinct intracellular effects than bortezomib and other common inhibitors binding to the proteasome active centers and rapidly blocking all forms of the protease. The rapamycin-like inhibitor will affect activity of free cores and the formation of new 26S assemblies. The cellular effects of such compound on the ubiquitin-dependent degradation will likely unfold slowly, which may help to at least delay drug resistance. Summarizing, the allosteric inhibitors affecting the proteasomal α face may constitute important tools to control proteasome catalytic activity and useful probes to test its molecular mechanism. These properties may put rapamycin-based compounds in the forefront of search for pharmacologically useful allosteric regulators of the ubiquitin proteasome pathway.

Authorship Contribution

Participated in research design: Osmulski and Gaczynska.

Conducted experiments: Osmulski and Gaczynska.

Performed data analysis: Osmulski and Gaczynska.

Wrote the manuscript: Osmulski and Gaczynska.

References

Adams, J. (2004). The proteasome: A suitable antineoplastic target. *Nat. Rev. Cancer* 4, 349–360.

Bajorek, M., Finley, D., and Glickman, M.H. (2003). Proteasome disassembly and downregulation is correlated with viability during stationary phase. *Curr. Biol.* 13, 1140–1144.

Banaszynski, L.A., Liu, C.W., and Wandless, T.J. (2005). Characterization of the FKBP-rapamycin-FRB ternary complex. *J. Am. Chem. Soc.* 127, 4715.

Cai, P., Tsao, R., and Ruppen, M.E. (2007). In vitro metabolic study of temsirolimus: Preparation, isolation, and identification of the metabolites. *Drug Metabol. Dispos.* 35, 1554–1563.

Ciechanover, A. (2012). Intracellular protein degradation: From a vague idea thru the lysosome and the ubiquitin-proteasome system and onto human diseases and drug targeting. *Biochim. Biophys. Acta Proteins Proteomics* 1824, 3–13.

Dick, L.R., and Fleming, P.E. (2010). Building on bortezomib: second-generation proteasome inhibitors as anti-cancer therapy. *Drug Discov. Today* 15, 243–249.

Dowling, R.J.O., Pollak, M., and Sonenberg, N. (2009). Current status and challenges associated with targeting mTOR for cancer therapy. *BioDrugs* 23, 77–91.

Da Fonseca, P., He, J., and Morris, E.P. (2012). Molecular Model of the Human 26S Proteasome. *Mol. Cell* 46, 54–66.

Gaczynska, M., and Osmulski, P.A. (2005). Small-molecule inhibitors of proteasome activity. *Methods in Molecular Biology* 301, 3–22.

Gaczynska, M., and Osmulski, P.A. (2011). Atomic force microscopy of proteasome assemblies. *Methods in Molecular Biology* (Clifton, N.J.) 736, 117–132.

Gaczynska, M., Osmulski, P.A., Gao, Y., Post, M.J., and Simons, M. (2003). Proline- and arginine-rich peptides constitute a novel class of allosteric inhibitors of proteasome activity. *Biochemistry* 42, 8663–8670.

Gao, Y., Lecker, S., Post, M.J., Hietaranta, A.J., Li, J., Volk, R., Li, M., Sato, K., Saluja, A.K., Steer, M.L., et al. (2000). Inhibition of ubiquitin-proteasome pathway-mediated IκBα degradation by a naturally occurring antibacterial peptide. *J. Clin. Invest.* 106, 439–448.

Goodey, N.M., and Benkovic, S.J. (2008). Allosteric regulation and catalysis emerge via a common route. *Nature* 4, 474–482.

Groll, M., Ditzel, L., Lowe, J., Stock, D., Bochtler, M., Bartunik, H.D., and Huber, R. (1997). Structure of 20S proteasome from yeast at 2.4 A resolution. *Nature* 386, 463–471.

Harrison, D.E., Strong, R., Sharp, Z.D., Nelson, J.F., Astle, C.M., Flurkey, K., Nadon, N.L., Wilkinson, J.E., Frenkel, K., Carter, C.S., et al. (2009). Rapamycin fed late in life extends lifespan in genetically heterogeneous mice. *Nature* 460, 392–395.

Huber, E.M., and Groll, M. (2012). The 19S cap puzzle: A new jigsaw piece. *Structure* 20, 387–388.

Iwanczyk, J., Sadre-Bazzaz, K., Ferrell, K., Kondrashkina, E., Formosa, T., Hill, C.P., and Ortega, J. (2006). Structure of the Blm10-20 S Proteasome Complex by Cryo-electron Microscopy. Insights into the Mechanism of Activation of Mature Yeast Proteasomes. *J. Mol. Biol.* 363, 648–659.

Jankowska, E., Gaczynska, M., Osmulski, P., Sikorska, E., Rostankowski, R., Madabhushi, S., Tokmina-Lukaszewska, M., and Kasprzykowski, F. (2010). Potential allosteric modulators of the proteasome activity. *Biopolymers* 93, 481–495.

Kleijnen, M.F., Roelofs, J., Park, S., Hathaway, N.A., Glickman, M., King, R.W., and Finley, D. (2007). Stability of the proteasome can be regulated allosterically through engagement of its proteolytic active sites. *Nature Struct. Mol. Biol.* 14, 1180–1188.

Lander, G.C., Estrin, E., Matyskiela, M.E., Bashore, C., Nogales, E., and Martin, A. (2012). Complete subunit architecture of the proteasome regulatory particle. *Nature* 482, 186–191.

Lasker, K., Förster, F., Bohn, S., Walzthoeni, T., Villa, E., Unverdorben, P., Beck, F., Aebersold, R., Sali, A., and Baumeister, W. (2012). Molecular architecture of the 26S proteasome holocomplex determined by an integrative approach. *Proc. Natl. Acad. Sci. U. S. A.* 109, 1380–1387.

Li, J., Post, M., Volk, R., Gao, Y., Li, M., Metais, C., Sato, K., Tsai, J., Aird, W., Rosenberg, R.D., et al. (2000). PR39, a peptide regulator of angiogenesis. *Nat. Med.* 6, 49–55.

Li, X., Wood, T.E., Sprangers, R., Jansen, G., Franke, N.E., Mao, X., Wang, X., Zhang, Y., Verbrugge, S.E., Adomat, H., et al. (2010). Effect of noncompetitive proteasome inhibition on bortezomib resistance. *J. Natl. Cancer Inst.* 102, 1069–1082.

Liang, J., Choi, J., and Clardy, J. (1999). Refined structure of the FKBP12-rapamycin-FRB ternary complex at 2.2 √Ö resolution. *Acta Crystallogr. Sect. D Biol. Cryst.* 55, 736.

Liu, C.W., Corboy, M.J., DeMartino, G.N., and Thomas, P.J. (2003). Endoproteolytic activity of the proteasome. *Science*. 299, 408–411.

Meyer, S., Kohler, N.G., and Joly, A. (1997). Cyclosporine A is an uncompetitive inhibitor of proteasome activity and prevents NF-κB activation. *FEBS Letters* 413, 354–358.

Ortega, J., Heymann, J.B., Kajava, A.V., Ustrell, V., Rechsteiner, M., and Steven, A.C. (2005). The axial channel of the 20S proteasome opens upon binding of the PA200 activator. *J. Mol. Biol.* 346, 1221–1227.

Osmulski, P.A., and Gaczynska, M. (2002). Nanoenzymology of the 20S Proteasome: Proteasomal Actions Are Controlled by the Allosteric Transition. *Biochemistry* 41, 7047–7053.

Osmulski, P.A., Hochstrasser, M., and Gaczynska, M. (2009). A Tetrahedral Transition State at the Active Sites of the 20S Proteasome Is Coupled to Opening of the α-Ring Channel. *Structure* 17, 1137–1147.

Pickering, A.M., Koop, A.L., Teoh, C.Y., Ermak, G., Grune, T., and Davies, K.J.A. (2010). The immunoproteasome, the 20S proteasome and the PA28αβ proteasome regulator are oxidative-stress-adaptive proteolytic complexes. *Biochem. J.* 432, 585–594.

Rabl, J., Smith, D.M., Yu, Y., Chang, S.-C., Goldberg, A.L., and Cheng, Y. (2008). Mechanism of Gate Opening in the 20S Proteasome by the Proteasomal ATPases. *Mol. Cell* 30, 360–368.

Rechsteiner, M., and Hill, C.P. (2005). Mobilizing the proteolytic machine: Cell biological roles of proteasome activators and inhibitors. *Trends Cell Biol.* 15, 27–33.

Smith, D.M., Kafri, G., Cheng, Y., Ng, D., Walz, T., and Goldberg, A.L. (2005). ATP binding to PAN or the 26S ATPases causes association with the 20S proteasome, gate opening, and translocation of unfolded proteins. *Mol. Cell* 20, 687–698.

Tan, X., Osmulski, P.A., and Gaczynska, M. (2006). Allosteric regulators of the proteasome: Potential drugs and a novel approach for drug design. *Current Medicinal Chemistry* 13, 155–165.

Unno, M., Mizushima, T., Morimoto, Y., Tomisugi, Y., Tanaka, K., Yasuoka, N., and Tsukihara, T. (2002). Structure determination of the constitutive 20S proteasome from bovine liver at 2.75 A resolution. *J. Biochem.* 131, 171–173.

Vignot, S. (2005). mTOR-targeted therapy of cancer with rapamycin derivatives. *Ann. Oncol.* 16, 525–537.

Whitby, F.G., Masters, E.I., Kramer, L., Knowlton, J.R., Yao, Y., Wang, C.C., and Hill, C.P. (2000). Structural basis for the activation of 20S proteasomes by 11S regulators. *Nature* 408, 115–120.

Footnotes

b) Reprint requests should be directed to:

Maria Gaczynska, Ph.D.

Institute of Biotechnology, UTHSCSA

15355 Lambda Drive,

San Antonio, TX, 78245

E-mail: Gaczynska@uthscsa.edu

Legends for Figures

Fig. 1 Types of the proteasome assemblies:

[A] the catalytic core proteasome (CP, 20S), side and top views, based on 1ryp crystal structure (Groll et al., 1997). The tube-shaped core is built from 28 subunits arranged in four heptameric rings (α–β–β–α). Three pairs of active sites harbored by β rings are concealed inside the gated tube. Substrates reach the centers through a gate formed by the noncatalytic α subunits. The gate area and grooves on the surface of α ring (α face) are marked by asterisk and small rings, respectively. The grooves are utilized for binding regulatory assemblies: PA200, 11S and 19S.

[B] The assembly of PA200-20S-PA200. The shape of PA200 module is based on the crystal structure 3L5Q. Below: the amino acid sequence of human tPA200 peptide with HbYX motif underlined (Iwanczyk et al., 2006; Ortega et al., 2005).

[C] The "activated proteasome" 11S-20S-11S. The shape of 11S module follows the crystal structure 1fnt (Whitby et al., 2000) of 20S core in complex with heptameric PA26, a homolog of mammalian PA28/REG.

[D] 26S assembly (19S-20S-19S). The shape of 19S assembly is derived from the cryoEM structure and molecular modeling (Da Fonseca et al., 2012; Lander et al., 2012; Lasker et al., 2012). The catalytic core shape is based on the 1ryp crystal structure. Below: the amino acid sequence of human tRpt5 peptide with HbYX motif underlined.

Fig. 2 Structures of the compounds tested in the study:

[A] the canonical structure of rapamycin (sirolimus) with binding and effector domains marked by brackets (Liang et al., 1999). R_1 (red) designates the functional group attached to carbon-40 and distinguishing rapamycin from its synthetic analogs (rapalogs; below).

[B] Single-domain rapamycin mimics. R_1 (red) and R_2 (blue) designate functional groups of FK-506 and pimecrolimus (below).

[C] *Seco*-rapamycin, the first physiological open ring metabolite of rapamycin. The red dashed line marks breaking of the lactone ring.

[D] Inhibitors of mTOR kinase structurally and mechanistically unrelated to rapamycin: PI-103 (left) and NVP-BEZ235 (right).

Fig. 3 Rapamycin inhibits degradation of casein by 20S proteasome. Casein fluorescently labeled with BODIPY was incubated with the human housekeeping core particle for up to 8 hrs and progress of its digest was monitored by measuring the increase of BODIPY fluorescence.

Fig. 4 Rapamycin inhibits [A, D] the post-hydrophobic (ChT-L) and [B, E] PGPH peptidases, and [C, F] activates the T-L peptidase of human core proteasomes. The Lineweaver-Burk plots of the control and rapamycin-treated proteasomes are shown in panels A-C. The data followed the mixed inhibition model for the post-hydrophobic cleavages, with $R^2 = 0.958$. The corresponding Michaelis constant K_M was 55.3 μM and $K_i = 0.49$ μM. For the PGPH activity the corresponding values were $R^2 = 0.978$, $K_M =$

173 µM, and K_i = 0.25 µM. The activation of the post-basic peptidase was of nonessential type. The dose response curves are presented in panels D-F. The single-domain derivative of rapamycin, FK-506, and the linear metabolite of rapamycin, seco-rapamycin, inhibit the ChT-L [D] and PGPH [E] peptidases, and activate the T-L [F] peptidase. The corresponding IC_{50} values are listed in Table 1. Means ± SD (n=3-5) or results of representative experiments are presented.

Fig. 5 Rapamycin and its derivatives affect conformational dynamics of the proteasome α face.

[A] AFM images of 20S proteasomes reveal the presence of two conformations: with smooth, convex α face ("closed") or with a dip (a darker spot) in the central area of α face ("open"). The leftmost panel presents a fragment of a field with imaged control proteasomes. Enlarged images of two top-view particles from the panel are presented on the right. Below the zoomed-in images there are corresponding sections through the topmost 1 nm part of the α ring, as marked on the contour of the core proteasome on the bottom-right. The diagrams between the field fragment and the single molecule images demonstrate how the central sections in four directions (a – d) were carried out through the images to distinguish between closed and open conformers. In short, a particle is classified as closed if all four sections are convex, as in the case of particle "1". If all four sections are concave instead of convex, a particle is classified as open, as in the case of particle "2". The grey scale bar on the far right represents the height of the particles, from the baseline (black) to the top (white). The same height scale applies to single molecule images in [B].

[B] A gallery of zoomed-in images of control, DMSO - treated human proteasomes (top) and proteasomes treated with 0.2 µM - 5 µM of rapamycin (bottom). The last three control images and the last six images of rapamycin – treated proteasomes represent particles in open conformation.

[C] Treatment with rapamycin (rapa) promotes changes in conformational dynamics of proteasome particles. Single particle analysis was applied to images of proteasomes in continuously scanned fields, with a single scan lasting for nearly 3 minutes. Open and closed conformers are represented by open and black-filled circles, respectively. Each row in the diagrams represents a single proteasome particle imaged in consecutive scans of the same area. Each column represents particles from a single field. The top diagram represents four particles treated with 10 µM rapamycin. The bottom diagram represents four particles treated with 10 µM rapamycin, and then with the model substrate for the ChT-L peptidase (SucLLVY-MCA; 100 µM). All the particles retain the ability to switch between open and closed conformations.

[D] Treatment of proteasomes with increasing concentrations of rapamycin results in decreasing ChT-L peptidase activity and decreasing content of closed conformers. Mean values ± SD are presented for n=3 experiments (activity) or n=10-14 fields with 100-300 proteasome particles (partition of conformers). Differences in the % of closed conformers between control and each of the rapamycin-treated samples are statistically significant ($p < 0.001$).

[E] Proteasomes treated with a saturating concentration (10 µM) of distinct rapamycin-related compounds display undistinguishable partition of conformers and are refractory to conformational shift induced by a peptide substrate (SucLLVY-MCA; 100 µM). The

partition of conformers in proteasomes incubated with PI-103 (10 μM) and then with the substrate was not significantly different from control and amounted for 74% ± 4% of closed particles (PI-103) vs. 29% ± 5% (PI-103, SucLLVY-MCA). Means values ± SD; n=8-22 fields with 100-500 particles. The differences between the partition for control proteasomes +substrate and proteasomes pretreated with rapamycin related compounds before adding substrate are statistically significant (p<0.001). Rapa=rapamycin, pimecro=pimecrolimus.

[F] Peptidase activities of proteasomes display varied sensitivity to treatment with a saturating concentration (10 μM) of distinct rapamycin-related compounds. The columns are grouped to point out the differences: the two-domain rapamycin stands out as the best inhibitor of the post-hydrophobic (ChT-L) peptidase, whereas both two-domain and one-domain derivatives strongly inhibit the post-acidic (PGPH) cleavages. Means values ± SD; n=2 or 3 experiments.

Fig. 6 Rapamycin interferes with activation of the 20S core by selected protein and peptide ligands of the α face. The relative ChT-L peptidase activity is presented as per cent of the control (20S with DMSO solvent). Specific activity of the control proteasome was in the range of 0.15 to 0.26 nanomoles of the AMC product released by mg of the 20S per second (0.20 ± 0.03 nanomol of AMC/mg per sec; n=23). Values of mean ± SD from n = 3 to 7 independent experiments are presented. Five μM rapamycin (RAPA) and 10 μM tRpt5 and tPA200 peptides were used, except in experiments with tPA200 where both compounds were used at 10 μM. 19S or 11S protein complexes were used in the 1:1 molar ratio with 20S. The differences between samples without and with
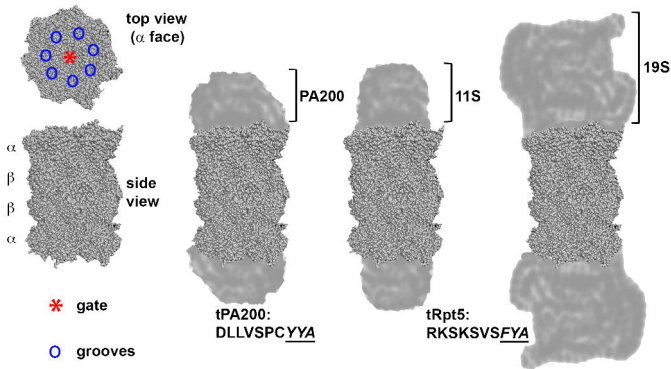
rapamycin added were statistically significant (p<0.01) except for the samples liganded

with 11S activator (green columns).

Table 1

Rapamycin and related compounds affect peptidase activities of the 20S proteasome in sub-micromolar to low-micromolar concentrations.
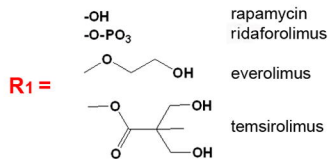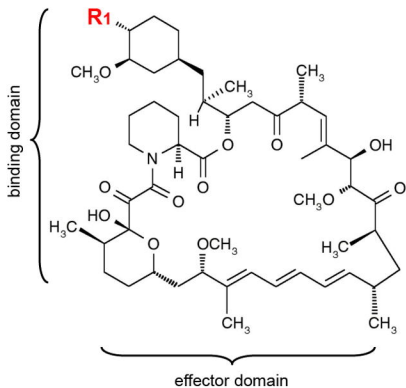
IC_{50} values (a drug concentration causing 50% inhibition of the indicated enzymatic activity) were calculated for ChT-L and PGPH peptidases. K_d (dissociation constant) and B_{max} (maximal activation effect achieved; in per cent above the control activity) values were calculated for the T-L peptidase. Mean ± SD from n = 2 or 3 experiments, or data from representative experiments set in duplicates or triplicates, are presented in the table. All three peptidase activities changed by no more than ± 20%, without a concentration-dependent trend, upon treatment with up to 10 μM of PI-103 or NVP-BEZ235, rapamycin unrelated mTOR inhibitors, in two independent experiments.

COMPOUND	IC_{50} [μM]: ChT-L	IC_{50} [μM]:: PGPH	K_d [μM]: T-L	B_{max} [%]: T-L
rapamycin	1.9 ± 0.2	0.41 ± 0.03	0.14	83
temsirolimus	2.1 ± 0.2	0.36 ± 0.03	0.19	81
everolimus	2.5 ± 0.7	0.48 ± 0.11	0.07	93
ridaforolimus	2.9 ± 0.5	0.43 ± 0.11	0.11	114
pimecrolimus	>20	0.57 ± 0.12	1.82	483
FK-506	>20	0.93 ± 0.04	1.14	257
seco-rapamycin	>20	6.45 ± 0.78	5.33	77

[A] 20S

[B] 20S+PA200

[C] 20S+PA26

[D] 20S+19S (26S)

top view (α face)

side view

α
β
β
α

PA200

11S

19S

* gate

○ grooves

tPA200: DLLVSPC*YYA*

tRpt5: RKSKSVS*FYA*

Figure 1

[A] Rapamycin and rapalogs

binding domain

effector domain

$R_1 =$

-OH	rapamycin
-O-PO$_3$	ridaforolimus
(methoxyethyl) -O—/\/O—OH	everolimus
(ester)	temsirolimus

[B] Single-domain mimics

$R_1 =$
- -OH FK-506
- -Cl pimecrolimus

$R_2 =$
- =CH$_2$ FK-506
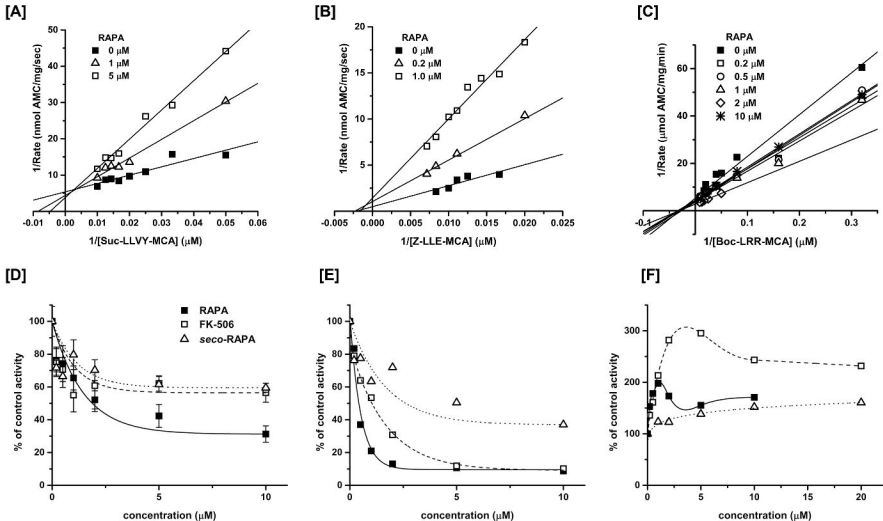- -H pimecrolimus
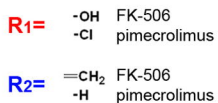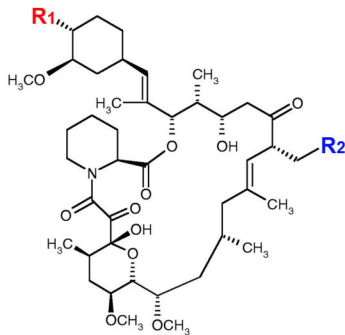
[C] Seco-rapamycin
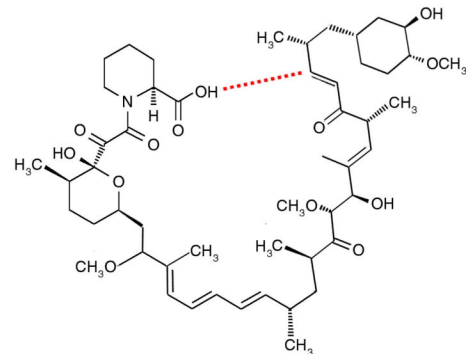
[D]
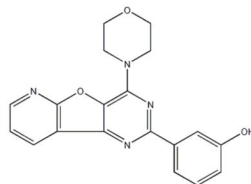
PI-103   **NVP-BEZ235**
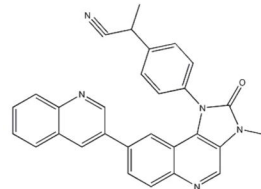
Figure 2
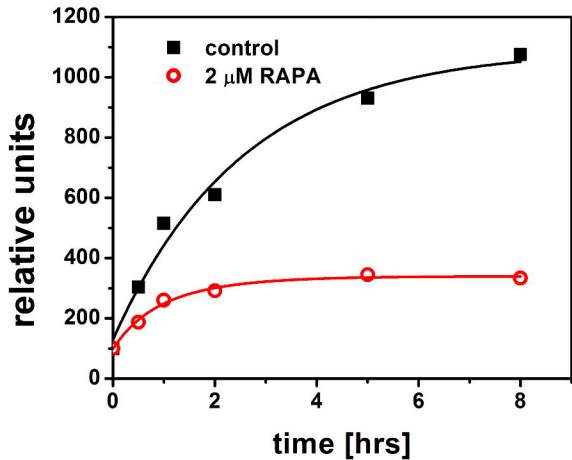
Figure 3

Figure 4

Figure 5

Figure 6